Molecular Crystals and Liquid Crystals
Publication details, including instructions for authors and subscription information:
http://www.tandfonline.com/loi/gmcl20

Efficient Red Organic Light-Emitting Diodes Using 2-(2-(4-Pentylbicyclo[2.2.2]octan-1-yl)-6-(2-(1,1,7-trimethyl-7-triphenysiliyllethyl-1,2,3,5,6,7-hexahydropyrido[3,2,1-ij]quinolin-9-yl)vinyl)-4H-pyran-4-ylidene)malononitrile as a Fluorescent Red Emitter

Bo Min Seo [a], Ji Hoon Seo [a], Jun Ho Kim [a], Jung Sun Park [a], Kum-Hee Lee [a], Min Hye Park [a], Seung Soo Yoon [b] & Young Kwan Kim [a]

[a] Department of Information Display, Hongik University, Seoul, 121-791, Korea

[b] Department of Chemistry, Sungkyunkwan University, Suwon, Gyungi-do, 440-746, Koea

Version of record first published: 18 Oct 2011

To cite this article: Bo Min Seo, Ji Hoon Seo, Jun Ho Kim, Jung Sun Park, Kum-Hee Lee, Min Hye Park, Seung Soo Yoon & Young Kwan Kim (2011): Efficient Red Organic Light-Emitting Diodes Using 2-(2-(4-Pentylbicyclo[2.2.2]octan-1-yl)-6-(2-(1,1,7-trimethyl-7-triphenysiliyllethyl-1,2,3,5,6,7-hexahydropyrido[3,2,1-ij]quinolin-9-yl)vinyl)-4H-pyran-4-ylidene)malononitrile as a Fluorescent Red Emitter, Molecular Crystals and Liquid Crystals, 550:1, 233-239

To link to this article: http://dx.doi.org/10.1080/15421406.2011.599758

Mol. Cryst. Liq. Cryst., Vol. 550: pp. 233–239, 2011

ISSN: 1542-1406 print/1563-5287 online
DOI: 10.1080/15421406.2011.599758

Efficient Red Organic Light-Emitting Diodes Using 2-(2-(4-Pentylbicyclo[2.2.2]octan-1-yl)-6-(2-(1,1,7-trimethyl-7-triphenysiliyllethyl-1,2,3,5,6,7-hexahydropyrido[3,2,1-ij]quinolin-9-yl)vinyl)-4H-pyran-4-ylidene)malononitrile as a Fluorescent Red Emitter

BO MIN SEO,[1] JI HOON SEO,[1] JUN HO KIM,[1]
JUNG SUN PARK,[1] KUM-HEE LEE,[1] MIN HYE PARK,[1]
SEUNG SOO YOON,[2] AND YOUNG KWAN KIM[1,*]

[1]Department of Information Display, Hongik University, Seoul 121-791, Korea
[2]Department of Chemistry, Sungkyunkwan University, Suwon, Gyungi-do 440-746, Koea

The authors have demonstrated red organic light-emitting diodes (OLEDs) using a new fluorescent red emitter, 2-(2-(4-pentylbicyclo[2.2.2]octan-1-yl)-6-(2-(1,1,7-trimethyl-7-triphenysiliyllethyl-1,2,3,5,6,7-hexahydropyrido[3,2,1-ij]quinolin-9-yl)vinyl)-4H-pyran-4-ylidene)malononitrile (DCJTPSO), achieved the maximum external quantum efficiency (EQE) of 2.06%, current efficiency (CE) of 3.83 cd/A, and Commision Internationale De L'Eclairage ($CIE_{x,y}$) coordinates of (0.58, 0.40) at 0.029 mA/cm^2 in comparison with control device using 4-(dicyanomethylene)-2-tert-butyl- 6-(1,1,7, 7-tetramethyljulolidin-4-yl-vinyl)- 4H-pyran which showed the maximum EQE of 1.07%, CE of 1.41 cd/A and $CIE_{x,y}$ coordinates of (0.61, 0.38) at 0.11 mA/cm^2. This result showed that the high performance of red device using DCJTPSO showed easier electron trapping directly on the emitter molecule.

Keywords light-emitting diode; Red organic lighting emitting diodes; 2-(2-(4-pentylbicyclo[2.2.2]octan-1-yl)-6-(2-(1,1,7-trimethyl-7-triphenysiliyllethyl-1,2,3,5,6,7-hexahydropyrido[3,2,1-ij]quinolin-9-yl)vinyl)-4H-pyran-4-ylidene)malononitrile; charge carrier trapping directly

Introduction

Since the first application of a multilayer structure in organic light-emitting diodes (OLEDs) by Tang and Vanslyke, OLEDs have attracted considerable interest due to their easy processability, flexibility, thinness, low operating voltages, high resolution, wide viewing angles, and fast response time [1]. So OLED have become a technology for the next generation full color flat-panel displays [2–7]. Many researchers have investigated fluorescent and phosphorescent green emitters for high device performance in OLED [8, 9]. However, the fluorescent red and blue emitters have remained to be weaker part in realizing the full color

*Corresponding author. E-mail: kimyk@hongik.ac.kr

display with low efficiency and dissatisfied color purity. Therefore, red emitters are still rare. In this paper, a new red fluorescent material,2-(2-(4-pentylbicyclo[2.2.2]octan-1-yl)-6-(2-(1,1,7-trimethyl-7-triphenysiliyllethyl-1,2,3,5, 6,7-hexahydropyrido[3,2,1-ij]quinolin-9-yl)vinyl)-4H-pyran-4-ylidene)malononitrile (DCJTPSO) was sythesized and studied. The optimized fluorescent red device using DCJTPSO achieved the maximum external quantum efficiency (EQE) of 2.06%, Current efficiency (CE) of 3.83 cd/A, and Commision Internationale De L'Eclairage ($CIE_{x,y}$) coordinates of (0.58, 0.40) at 0.029 mA/cm^2, respectively.

Experimental

Synthesis

Synthesis of (*N*-2-ethylhexyl)-3(6)-phenothiazinylene vinylene-*co*-9,10-anthrylene vinylene) (KPD-1). Firstly *N*-(2-ethylhexyl)phenothiazine (EHPZ) was synthesized from the reaction of phenothiazine (6 g, 0.03 mol) and 2-ethylhexylbromide (5.8 g, 0.03 mol) in the presence of sodium hydroxide (7.2 g, 0.18 mol) in dimethylsulfoxide (60 ml) at room temperature for 3 h.[11] Yield: 73%. ^{1}H NMR($CDCl_3$), δ: 6.87, 7.12 (m, 8H, Ar-***H***), 3.70 (m, 2H, N-C***H***$_2$-), 1.93 (t, 1H, C***H***-), 1.22–1.44 (m, 9H, -C***H***$_2$-), 0.83–0.87 (m, 6H, -C***H***$_3$), IR (KBr), cm^{-1}: 3064 (Ar CH), 2926 (aliphatic CH), 2857 (N-CH_2-), 1593, 1485 (Ar C=C).

N-(2-Ethylhexyl)-3(6)-formylphenothiazine (EHFZ) was synthesized using modified Vilsmeier-Haack formylation in the second step [6, 7]. Yield : 45%, ^{1}H NMR($CDCl_3$), δ: 9.73 (m, 2H, aldehydic hydrogen), 6.88, 7.56 (m, 6H, Ar ***H***), 3.73 (t, 2H, N-C***H***$_2$-), 1.17–1.85 (m, 9H, -C***H***$_2$-, C***H***-), 0.76–0.82 (m, 6H, -C***H***$_3$), IR (KBr), cm^{-1}: 3048 (Ar CH; weak signal), 2927 (aliphatic CH), 2857 (N-CH_2-), 2724 (aldehydic hydrogen), 1688 (C=O), 1600, 1465 (Ar C=C).

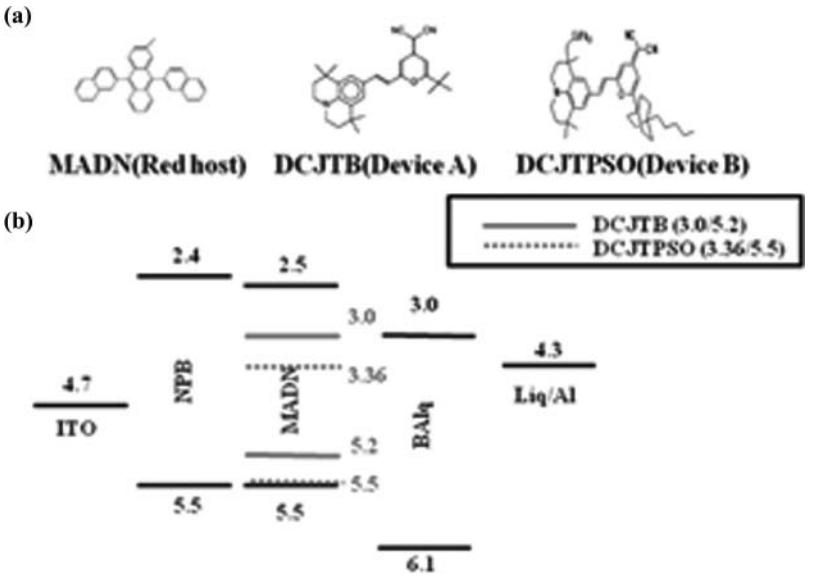

Figure 1. (a) Molecular structure of the key materials used for fabrication. (b) The energy diagram of the red OLEDs in this study.

9,10-(Chloromethyl)anthracene (4.8 g, 0.014 mol) was reacted with triethylphosphite (30g, 0.18 mol) at 120°C for 12 h. The unreacted triethylphosphite was removed under reduced pressure.[12] 9,10-Bis(diethoxyphosphinylmethyl)antrhracene (PHAN) was obtained as yellow crystal. Yield: 92%. ^{1}H NMR ($CDCl_3$), δ: 7.57, 8.38 (m, 8H, Ar ***H***), 4.23 (d, 8H, -C***H***$_2$O-P-), 3.84 (m, 4H, Ar-C***H***$_2$-P), 1.06 (t, 12H, -C***H***$_3$), IR (KBr), cm-1: 3026 (Ar CH), 2983 (aliphatic CH), 1251 (P=O).

As presented in Scheme 1 (a), KPD-1 was synthesized with adding potassium *tert*-butoxide (4.73 g, 0.04 mol) solution into a mixture of EHFZ (1.70 g, 0.005 mol) and PHAN (1.20g, 0.0025 mol) in THF, and then stirring at room temperature for 7 h. Yield: 51%, ^{1}H NMR ($CDCl_3$), δ: 6.94 (m, 4H, =C***H***-), IR (KBr), cm^{-1}: 3021 (Ar CH), 2924 (aliphatic CH), 2855 (N-CH_2-), 1578, 1471 (Ar C=C), 965 (trans vinylene).

Poly(BFMP$_{12}$-AV) alternating copolymer, as shown in Scheme 1 (b), was obtained by Horner-Emmons condensation reaction [5, 8, 9].

Fabrication of PLED

Indium tin oxide (ITO)-coated glass was cleaned in an ultrasonic bath by the following sequence: in acetone, methanol, distilled water and isopropyl alcohol. Thereafter, pre-cleaned ITO was treated by O_2 plasma with the conditions of 2×10^{-2} Torr, 125 W for 2 min. All devices were fabricated using the high vacuum (5×10^{-7} Torr) thermal evaporation of organic materials onto the surface of the ITO-coated glass substrate (15 Ω/sq, emitting area was 3 mm x 3 mm). The deposition rates were 1.0 ∼ 1.1 Å/sec for organic materials and 0.1 Å/sec for lithium quinolate (Liq), respectively. After the deposition of the organic layers without a vacuum break the Al cathode was deposited at a rate of 10 Å/sec. With the DC voltage bias, the optical and electrical properties of OLEDs such as the current density, luminance, CE, and electroluminescence (EL) spectra of the emission characteristics were measured with Keithley 236 and CHROMA METER CS-1000A instruments. The

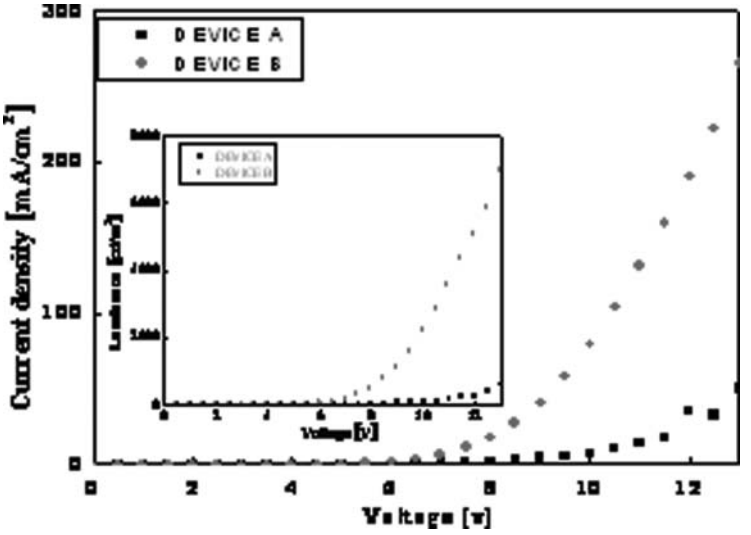

Figure 2. Current density versus voltage characteristics of device A and B. Inset: Luminance versus voltage characteristics of device A and B.

UV-Visible absorption spectra were measured in 1.2-dichloroethane solution (10^{-5} M) using a Shimadzu UV-1650PC. The photoluminescence (PL) were obtained in 1.2-dichloroethane solution (10^{-5} M) and thin film using an Amincobrowman series 2 luminescence spectrometer. The fluorescent quantum yields were determined in 1.2-dichloroethane solution at 293 K against 4-(dicyanomethylene)-2-tert-butyl-6-(1,1,7,7-tetramethyljulolidin-4-yl-vinyl)-4H-pyran (DCJTB) ($\Phi = 0.78$) as a reference. All measurements were carried out under ambient conditions at room temperature.

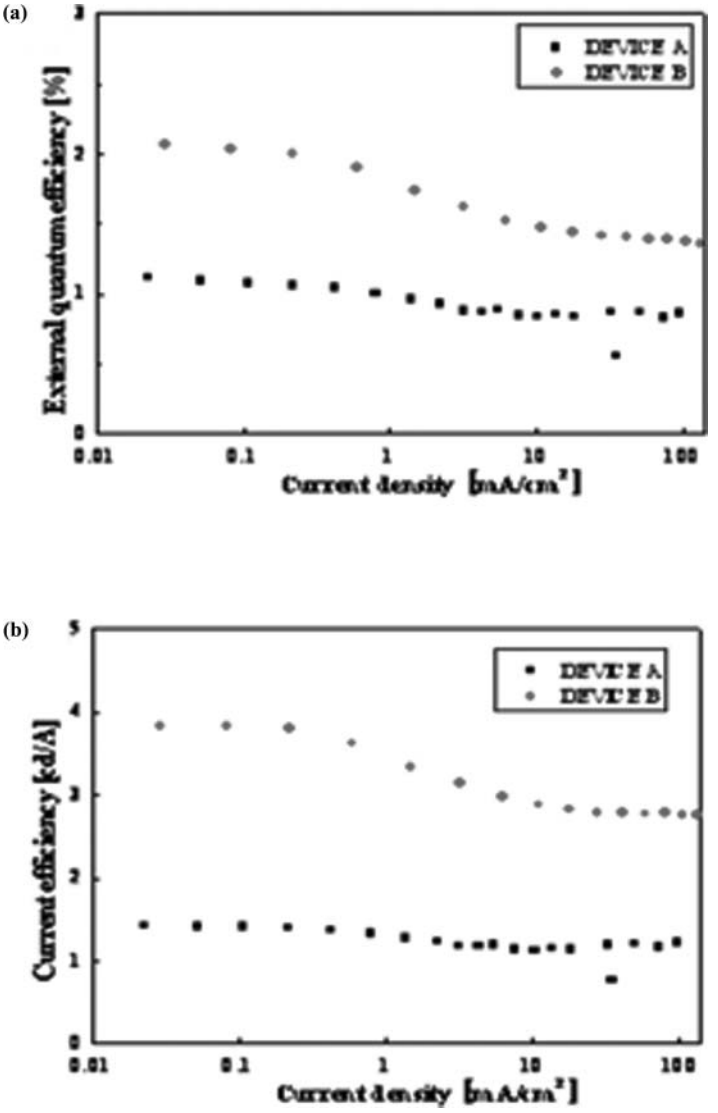

Figure 3. (a) EQE versus current density characteristics of device A and B. (b) CE versus current density characteristics of device A and B.

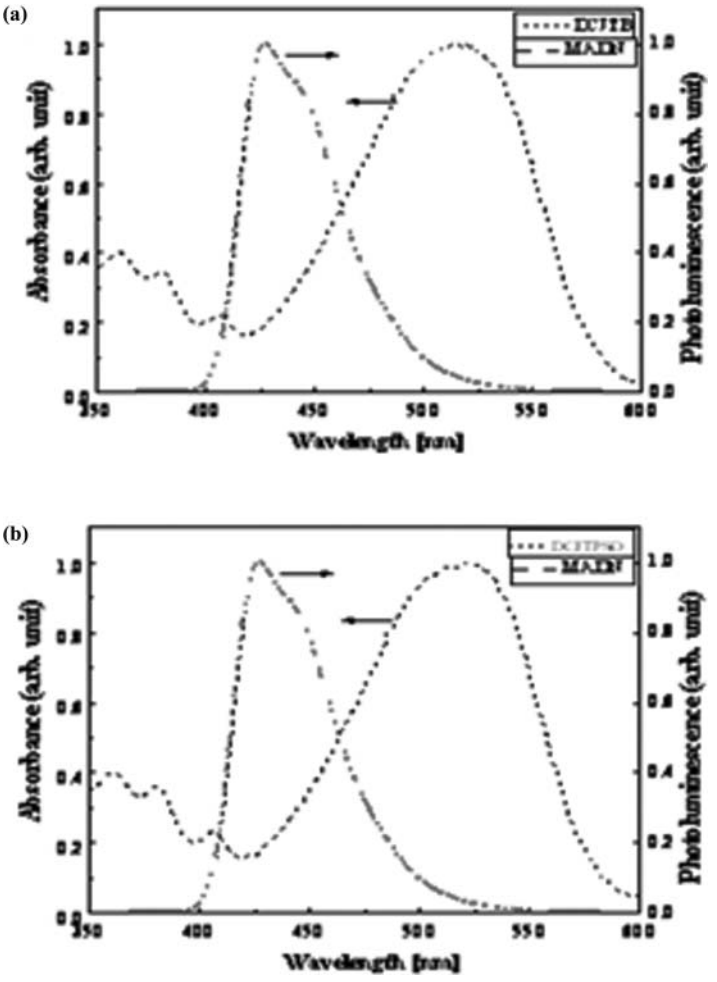

Figure 4. (a) UV/visible absorption spectrum of DCJTB and PL spectrum of MADN. (b) UV/visible absorption spectrum of DCJTPSO and PL spectrum of MADN.

Results and Discussion

Figure 1 (a) shows the molecular structure of key materials used for fabrication, 2-methyl-9, 10-di(2-naphthyl)anthracene (MADN), DCJTB (device A), and DCJTPSO (device B), respectively. Figure 1 (b) shows energy level diagram of two devices with the structure of ITO/N,N'-bis(naphthalen-1-yl)-N,N'-bis(phenyl)-benzidine (NPB) (500 Å)/DCJTB:MADN (300 Å, 5%, device A) or DCJTPSO:MADN (300 Å, 5%, device B)/bis-(2-methyl-8-quinolinolate)-4-(phenylphenolato)aluminium (BAlq) (300 Å)/Liq(20 Å)/Al(1000 Å), respectively. The doping concentrations of DCJTB and DCJTPSO in MADN were optimized to 5%, respectively. NPB, MADN, BAlq and Liq were used for hole transporting layer, red host, electron transporting layer (ETL), and electron injection layer, respectively. DCJTB and DCJTPSO were also used for fluorescent red emitter, respectively.

Figure 2 shows current density versus voltage characteristics of device A and B. Inset Fig 2 shows luminance versus voltage characteristics of device A and B. Device A and B

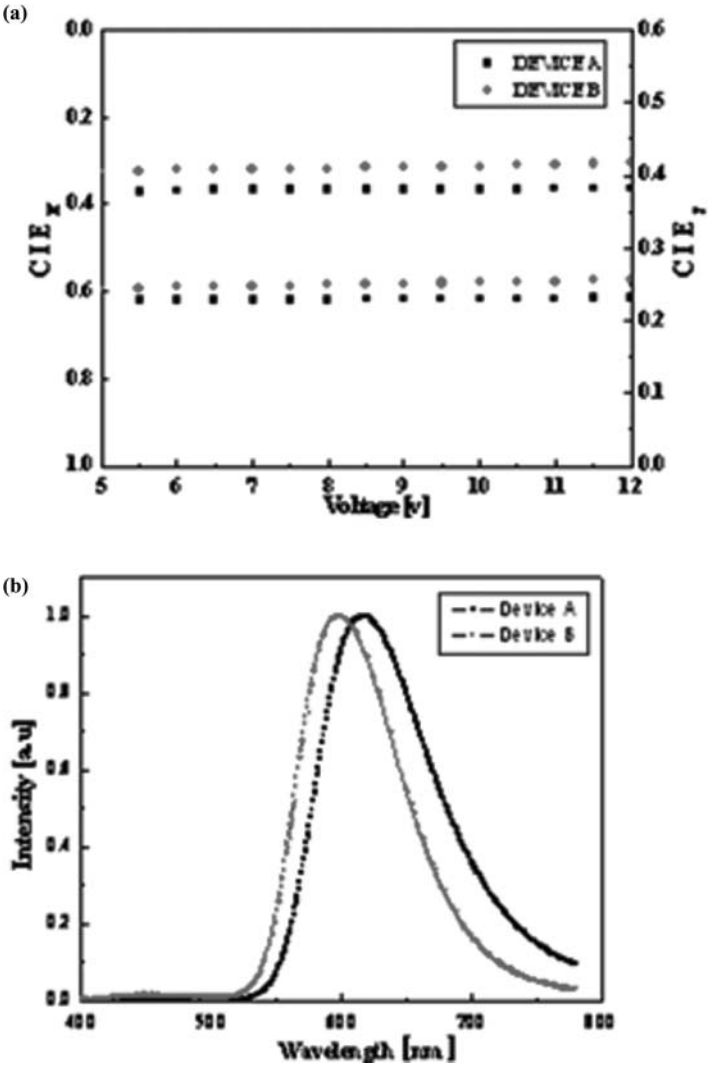

Figure 5. (a) $CIE_{x,y}$ coordinates versus voltage characteristics of device A and B from 5 to 12 V. (b) EL spectra of device A and B at 1000 cd/m^2.

showed the current density of 50.1 and 265 mA/cm^2 at 13 V, respectively. Seeing that the highest occupied molecular orbital and the lowest occupied molecular of red dopant, the carrier injection barrier are 0.5 eV for electrons and only 0 eV for holes. From the electron carrier point of view, there is the direct electron injection from the ETL to the red emitter. Also the red device B using DCJTPSO showed higher current density than that of the red device A with same device structure.

This result showed carrier injection of the devices B is better than that of the device A. Figure 3 (a) and (b) show the EQE and CE versus current density characteristics of two devices. Device A and B had a maximum EQE of 1.07 and 2.06% and CE of 1.41 and 3.83 cd/A at 0.11, 0.03 mA/cm^2, respectively. They also exhibited a EQE of 0.84 and 1.49% and CE of 1.13 and 2. 90 cd/A at 10 mA/cm^2, respectively.

Figure 4 (a) and (b) show the UV/visible absorption spectra of DCJTB (device A) and DCJTPSO (device B) and PL spectrum of MADN, respectively. The UV/visible absorption of DCJTPSO and PL spectra MADN showed almost the same spectra overlap in comparison of them of DCJTB and MADN. This result indicated similar efficient Förster singlet energy transfer from MADN to the red emitter.

However, PL quantum yield of DCJTPSO(0.97) showed higher than that of DCJTB(0.78). As a result, the performance of the red device B using the DCJTPSO is better performance than that of the red device A with same device structure.

Figure 5 (a) shows the $CIE_{x,y}$ coordinates changes of two devices from 5 to 12 V. Devices A and B showed $CIE_{x,y}$ coordinates of (0.61, 0.39) and (0.58, 0.41) at 13 and 9 V, respectively.

Figure 5 (b) shows the EL spectra of two devices at 1000 cd/m^2. Device A and B had a red peak at 615 and 601 nm for DCJTB and DCJTPSO, respectively. Device A showed more redwish emission than device B.

Conclusions

In this study, we demonstrated efficient red OLEDs using a new fluorescent red emitter, DCJTPSO. The optimaized red device using DCJTPSO showed higher EQE of 2 times and CE of 2.7 times than control red device using DCJTB. This result indicated similar efficient Förster singlet energy transfer from MADN to the red device using DCJTB or DCJTPSO because the UV/visible absorption of DCJTPSO and PL spectra MADN showed almost the same spectra overlap in comparison with them of DCJTB and MADN. However, PL quantum yield of DCJTPSO(0.97) showed higher than that of DCJTB(0.78). This process of device B on charge easier electron trapping directly on the emitter molecule also resulted in a more efficient performance than that of device A.

As a result, the performance of the red device B using the DCJTPSO is better than that of the red device A with same device structure.

Acknowledgment

This work was supported by 2009 Hongik University Reserch Fund and the ERC program of the Korea Science and Engineering Foundation (KOSEF) grant funded by the Korea Ministry of Education, Science and Technology (MEST) and (No. R11-2007-045-03001-0).

References

[1] C. W. Tang and S. A. VanSlyke, *Appl. Phys. Lett.* **51**, 913 (1987).
[2] J. Kido, K. Hongawa, K. Okuyama, and K. Nagai, *Appl. Phys. Lett.* **64**, 815 (1994).
[3] J. H. Seo, J. H. Kim, J. H. Seo, G. W. Hyung, J. H. Park, K. H. Lee, S. S. Yoon, and Y. K. Kim, *Appl. Phys. Lett.* **90**, 203507 (2007).
[4] Y. Sun, N. C. Giebink, H. Kanno, B. Ma, M. E. Thompson, and S. R. Forrest, *Nature*, **440**, 908 (2006).
[5] M. H. Ho, Y. S. Wu, S. W. Wen, M. T. Lee, T. M. Chen, C. H. Chen, K. C. Kwok, S. K. So, K. T. Yeung, Y. K. Cheng, and Z. Q. Gao, *Appl. Phys. Lett.* **89**, 252903 (2006).
[6] J. R. Sheats, H. Antoniadis, M. Hueschen, W. Leonard, J. Miller, R. Moon, D. Roitman, and A. Stocking, *Science* **273**, 884 (1996).
[7] L. Zhou, A. Wanga, S. Wu, J. Sun, S. Park, and T. N. Jackson, *Appl. Phys. Lett.* **88**, 083502 (2006).
[8] G. Yu, J. Cao, J. Hummelen, F. Wudl, and A. J. Heeger, *Science* **270**, 1789 (1995).
[9] G. Yu, Y. Cao, J. Wang, J. McElvain, and A. J. Heeger, *Synth. Met.* **102**, 904 (1999).